A Model Predictive Approach for Voltage Support in Microgrids using Energy Storage Systems

Niranjan Bhujel†, Astha Rai,
Timothy M. Hansen, and Reinaldo Tonkoski
South Dakota State University
Brookings, South Dakota, USA
Email: †niranjan.bhujel@jacks.sdstate.edu

Ujjwol Tamrakar
Sandia National Laboratories
Albuquerque, New Mexico, USA 87185

***Abstract*—Low voltage microgrid systems are characterized by high sensitivity to both active and reactive power for voltage support. Also, the operational conditions of microgrids connected to active distribution systems are time-varying. Thus, the ideal controller to provide voltage support must be flexible enough to handle technical and operational constraints. This paper proposes a model predictive control (MPC) approach to provide dynamic voltage support using energy storage systems. This approach uses a simplified predictive model of the system along with operational constraints to solve an online finite-horizon optimization problem. Control signals are then computed such that the defined cost function is minimized. By proper selection of MPC weighting parameters, the quality of service provided can be adjusted to achieve the desired performance. A simulation study in Matlab/Simulink validates the proposed approach for a simplified version of a 100 kVA, 208 V microgrid using typical parameters. Results show that performance of the voltage support can be adjusted depending on the choice of weight and constraints of the controller.**

***Index Terms*—Voltage control, voltage support, model predictive control, optimal control, microgrids.**

I. Introduction

Microgrids typically operate at low to medium voltage ranges; hence the R/X ratio is usually high [1], resulting in high voltage sensitivity to both active and reactive power. In this paper, the potential of utilizing energy storage systems (ESSs) to provide voltage support in microgrids is analyzed. Different methods of voltage control for microgrids have been proposed in the literature. Droop-based voltage control has been often used [2], [3] to provide voltage support to microgrids. Droop control ensures the sharing of load with multiple ESSs for voltage support. However, droop controllers can have oscillatory behavior and lead to sub-optimal performance. In [4], H-∞ based control has been proposed. Although this approach provides robust stability, a precise model of the system is required for proper implementation. Moreover, nonlinear constraints such as saturation are generally not well-handled. Another approach to providing voltage support is using linear quadratic regulators [5]. However, when deploying ESSs for voltage support, operational constraints such as inverter size, the rate at which the ESS can change its output, the limited power available for voltage support, etc., have to be incorporated into the formulation.

Model predictive control (MPC) can provide an ideal framework for voltage support in microgrids using ESSs while handling the aforementioned operational constraints. MPC has been proposed for voltage control of single phase microgrids [6] without considering the disturbance model. Without the disturbance model, the controller cannot make a correction when the disturbance acts on the system which results in offset in tracking and deteriorate the controller performance [7]. Another MPC approach for behind-the-meter energy storage for large distribution systems was proposed in [8], based on the computation of the cost-optimal dispatch. However, the fast voltage control dynamics were neglected, which can lead to undesirable transient oscillations or poor dynamic performance. In [9], MPC based PV-ESS system with voltage support capablity has been proposed. This approach address variable load demand, flexible power regulation, voltage support, etc. In [10], fast frequency support in microgrid using ESS has been presented. This approach incorporates different ESS constraints like lifetime, degradation, etc, implicitly. This approach looks only at frequency support.

In this paper, an MPC framework to provide voltage support for microgrids is proposed. Conventional controllers do not have the flexibility to consider the operating costs of ESSs (e.g., ESS lifetime degradation, cost, impact on stacked services, energy cost) needed to provide voltage support. The proposed MPC-based approach can include operational constraints and costs to optimally dispatch the ESS. Furthermore, this approach provides the flexibility to tune the controller to adjust the quality-of-service (QoS), i.e., performance of the controller. The proposed framework addresses the technical challenges associated with fast voltage dynamics, which can cause local power quality issues (e.g., voltage deviations, sympathetic over/under voltages).

The paper is organized as follows: Section II presents the simplified model used in the predictive controller for voltage dynamics of an isolated power system. In Section III, the proposed MPC approach is discussed. The methodology to validate the proposed approach is discussed in Section IV. The results and analysis are presented in Section V. Finally,

This work is supported by the U.S. Department of Energy under grant number DE-SC0020281, and National Science Foundation (NSF) grant numbers MRI-1726964 and OAC-1924302.

The work at Sandia (Ujjwol Tamrakar) is supported by the US Department of Energy, Office of Electricity, Energy Storage Program.

Sandia National Laboratories is a multi-mission laboratory managed and operated by National Technology and Engineering Solutions of Sandia, LLC., a wholly owned subsidiary of Honeywell International, Inc., for the U.S. Department of Energy National Nuclear Security Administration under contract DE-NA-0003525. This paper describes objective technical results and analysis. Any subjective views or opinions that might be expressed in the paper do not necessarily represent the views of the U.S. Department of Energy or the United States Government. SAND2021-2092 C

Section VI concludes the paper.

II. A Simplified Predictive Model of Voltage Dynamics in Microgrids

In this section, a simplified model representing the voltage dynamics of a microgrid system is derived. A simplified dynamic model of a microgrid was effectively used in a MPC to provide frequency support [10]. The proposed simplified model will be utilized within the proposed MPC framework as a "predictive" model to approximate the voltage in the system. It is important to note here that a simplified model is desirable to reduce the computational complexity of the controller, but control actions are applied to the full system model. The inherent feedback mechanism of the MPC framework can handle any mismatches that may result due to the use of this simplified model. A single line diagram of an inverter-based ESS connected to a microgrid is shown in Fig. 1. The inverter is modeled as an average current-controlled voltage source inverter (CC-VSI) while the grid is modeled by the Thevenin equivalent voltage v_g, and equivalent resistance and inductance R and L, respectively. At the point of common coupling (PCC), a capacitor C is added, which is part of the inverter filter. The voltage across the capacitor is represented by v_c. The system load is also connected at the PCC, which draws the current i_L. One thing to note here is that, the frequency dynamics and voltage controller dynamics of the microgrid are neglected since they are slower compared to network dynamics.

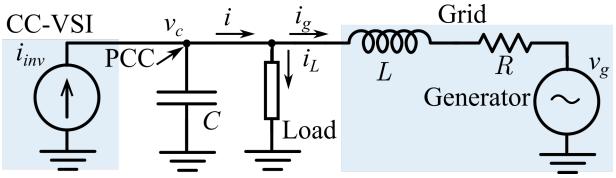

Fig. 1. Schematic representing an ESS connected to a microgrid. The ESS is represented as CC-VSI for modeling purposes.

The grid current i_g and capacitor voltage v_c can be described in the abc frame as:

$$\frac{di_{g,abc}}{dt} = \frac{v_{c,abc} - v_{g,abc} - i_{g,abc}R}{L} \tag{1}$$

$$\frac{dv_{c,abc}}{dt} = \frac{i_{inv,abc} - i_{g,abc} - i_{L,abc}}{C} \tag{2}$$

Applying Park's transformation and neglecting the zero component assuming a balanced system, the state-space representation of the system's voltage dynamics in $dq0$ frame is given by:

$$\dot{i}_{gd} = -\frac{R}{L}i_{gd} + \omega i_{gq} + \frac{v_{cd}}{L} - \frac{v_{gd}}{L} \tag{3a}$$

$$\dot{i}_{gq} = -\omega i_{gd} - \frac{R}{L}i_{gq} + \frac{v_{cq}}{L} - \frac{v_{gq}}{L} \tag{3b}$$

$$\dot{v}_{cd} = -\frac{i_{gd}}{C} + \omega v_{cq} + \frac{i_{invd}}{C} - \frac{i_{Ld}}{C} \tag{3c}$$

$$\dot{v}_{cq} = -\frac{i_{gq}}{C} - \omega v_{cd} + \frac{i_{invq}}{C} - \frac{i_{Lq}}{C} \tag{3d}$$

where ω represnts the rated frequency of microgrid system, i_{gd}, i_{gq}, v_{cd} and v_{cq} represents the states of the system, i_{invd} and i_{invq} represents input to the system, and v_{gd} and v_{gq} represent the d and q components of v_g, respectively, and i_{Ld} and i_{Lq} represents the d and q components of i_L which are modeled as a disturbance as it cannot be varied to achieve the control goal. It is important to note that the microgrid's Thevenin equivalent voltage v_g is estimated through a feed-forward term.

III. Proposed MPC Approach

A. Transformation of State Differential Equations

The system of equations (3) describes the voltage dynamics of a microgrid system. There are four state variables, but states i_{gd} and i_{gq} cannot be directly measured because in a real system the loads are distributed, and the impedance branch shown in Fig. 1 is an equivalent impedance. Instead, the inverter output current i shown in Fig. 1 can be measured and the state variables i_{gd} and i_{gq} can be recast in terms of i using the relationship $i_g = i - i_L$. Thus the following set of differential equations representing the system dynamics is obtained:

$$\frac{d}{dt}\begin{bmatrix} i_d \\ i_q \\ v_{cd} \\ v_{cq} \end{bmatrix} = \begin{bmatrix} -\frac{R}{L} & \omega & \frac{1}{L} & 0 \\ -\omega & -\frac{R}{L} & 0 & \frac{1}{L} \\ -\frac{1}{C} & 0 & 0 & \omega \\ 0 & -\frac{1}{C} & -\omega & 0 \end{bmatrix} \begin{bmatrix} i_d \\ i_q \\ v_{cd} \\ v_{cq} \end{bmatrix} + \begin{bmatrix} 0 & 0 \\ 0 & 0 \\ \frac{1}{C} & 0 \\ 0 & \frac{1}{C} \end{bmatrix} \begin{bmatrix} i_{invd} \\ i_{invq} \end{bmatrix} + \begin{bmatrix} -\frac{1}{L} & 0 \\ 0 & -\frac{1}{L} \\ 0 & 0 \\ 0 & 0 \end{bmatrix} \begin{bmatrix} v_d \\ v_q \end{bmatrix} \tag{4}$$

where $v_d = v_{gd} + \omega L i_{Lq} - R i_{Ld} - L\frac{di_{Ld}}{dt}$ and $v_q = v_{gq} - \omega L i_{Ld} - R i_{Lq} - L\frac{di_{Lq}}{dt}$. Here, v_d and v_q are the d and q components respectively of Thevenin's equivalent voltage of combined grid and load. These variables cannot be measured directly and must be estimated. The discussion regarding the estimator is out of scope of this paper. For this paper, the first two equations from (4) are used to calculate v_d and v_q. Derivative on the left-hand side (i.e., of i_d and i_q) of the equations are calculated using data from current and previous sample instant. This approach is valid if the measurement noise is low, otherwise, estimators must be used. Also, this paper assumes that the Thevenin equivalent impedance at the point of interconnection of the inverter is known. If this information is unknown or, if grid conditions change, different online parameter estimation techniques can be applied [10]. In addition, it is important to note that the d component of current is proportional to active power, whereas q is proportional to negative of reactive power. Thus, d and q components of the current can be seen as a proxy for active and reactive power to provide proper voltage support.

B. MPC Formulation

The continuous-time state equation derived in (4) can be discretized in the following form:

$$x_{k+1} = F(x_k, u_k, u_{dk}) \tag{5}$$

where, at discrete instant k, $x_k = [i_{dk}, i_{qk}, v_{cdk}, v_{cqk}]^\top$ represents the states, $u_k = [i_{invd_k}, i_{invq_k}]^\top$ is the control inputs, and $u_{dk} = [v_{dk}, v_{dk}]^\top$ is the disturbances to the system.

Let N be the horizon length and T_s be the sample time. The objective of the controller is to support voltage at PCC v_c. For simplicity, we can choose v_c to align with one of the d or q axes. For this paper, axes are selected such that d-axis aligns with v_c, and thus only v_{cd} needs to be controlled as v_{cq} is zero. To support the voltage, i_{invd} and i_{invq} are utilized to provide active and reactive power support because both can support the voltage. However, their costs differ as reactive power support does not use ESS energy (except to compensate for losses). Optimal values of the control actions i_{invd} and i_{invq} to support the voltage at any given time are computed by the MPC based on the relative weights provided to each term in the formulation. Let us assume $\Gamma = \{1, 2, ..., N\}$ represents the set of sample instant in the forward horizon. Here, v_{cdk} represents the variable that needs to be controlled at discrete sample instant k and Δv_{cdk} represents the voltage deviation from the reference value in per unit. The reference voltage is set internally in the controller., then MPC can be formulated as:

$$\min_{i_{invd}, i_{invq}} \quad J_\Gamma = \sum_{k=1}^{N} ||\Delta v_{cdk}||_Q^2 + \sum_{k=1}^{N-1} ||u_k||_S^2 \tag{6a}$$

subject to

$$x_{k+1} = F(x_k, u_k, u_{dk}) \ \forall \ k \in \Gamma - \{N\} \tag{6b}$$

$$|i_{invd_k}| \leq I_{d,max} \ \forall \ k \in \Gamma \tag{6c}$$

$$|i_{invq_k}| \leq I_{q,max} \ \forall \ k \in \Gamma \tag{6d}$$

$$|i_{invd_{k+1}} - i_{invd_k}| \leq S_d \ \forall \ k \in \Gamma - \{N\} \tag{6e}$$

$$|i_{invq_{k+1}} - i_{invq_k}| \leq S_q \ \forall \ k \in \Gamma - \{N\} \tag{6f}$$

where $||a||_A^2 = a^\top A a$ is the norm of vector a with respect to matrix A, $I_{d,max}$ and $I_{q,max}$ are the limits on d and q components of inverter current, respectively, and S_d and S_q are the ramp rate limits on i_{invd} and i_{invq}, respectively. The system dynamics are incorporated in (6b) as a constraint. J_Γ is the cost function that needs to be minimized. The cost function represents a numerical value of a penalty. The first term can be subjectively interpreted as the cost of the voltage deviation. The second term can be interpreted as the cost of using active and reactive power to achieve the control goal. These costs vary depending upon the requirements and available energy. Q and S are weighting matrices corresponding to the output that needs to be controlled and control input, respectively. Here, the control input (i_{invd} and i_{invq}) that corresponds to inverter power are supplied from ESS. The ESS capacity is neglected, since the inverter is operating on the voltage support function. Inverter current ramp rate limits along with weight matrix S can be used to address ESS life time, degradation issue. All the variables are converted to per unit before entering the cost function. Improved quality-of-service may come at the cost of inverter power (both active and reactive power). The cost function is defined such that cost on the inverter power and the degradation of the transient performance is included in the formulation. Depending on the cost of the control

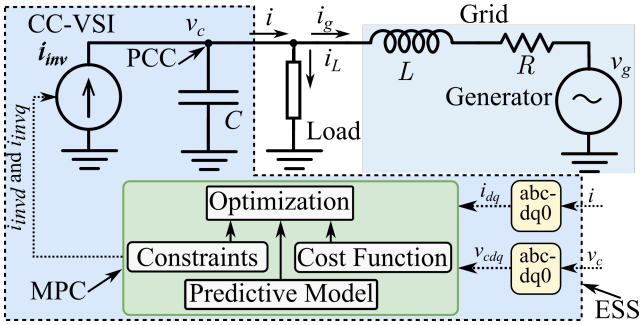

Fig. 2. Simulation setup of the system with the MPC.

effort and the desired transient performance, the weighting matrices Q and S can be tuned. The Q matrix can be used to penalize poor system performance (i.e., to penalize Δv_{cd}), while the S matrix can be used to penalize the control effort (i.e., the current output from the inverter). In this case, the weighting matrix Q has a single element, Q_{11}. Similarly, S is a 2×2 matrix defined as $diag(S_{11}, S_{22})$. Solving this optimization problem over the time horizon Γ results in the following solution $i^*_{invd} = \{i^*_{invd_1}, i^*_{invd_2}, ..., i^*_{invd_N}\}$ and $i^*_{invq} = \{i^*_{invq_1}, i^*_{invq_2}, ..., i^*_{invq_N}\}$. With the first term of these two sequences used as the control signal in the next sample instant, this gives the following control law:

$$i_{invd} = i^*_{invd_1}, \ i_{invq} = i^*_{invq_1} \tag{7}$$

IV. Simulation Setup

The simulation study was carried out using the setup illustrated in Fig. 2 using MATLAB/Simulink. The microgrid considered is a 100 kVA, 208 V three-phase microgrid system. A variable load is connected at the PCC, which is used to generate step load changes that result in voltage deviations in the system. In addition, the step changes in the voltage v_g were also used to characterize the performance of the proposed approach. The system parameters and MPC settings used in this study are summarized in Table I. Equation (4) was discretized using *Runge-Kutta* method of order 4. The sample time was selected based on time constants of the system that comes from the eigenvalues of state matrix [11]. In [10], applicability of MPC for smaller time scale has been shown. A standard Simulink phase-locked loop block was used to extract the instantaneous phase angle of v_c (reference) to transform abc variables into $dq0$ variables. These transformed variables are used as measurements for the MPC. Given these measurements, the MPC computes the optimal value of inverter currents i_{invd} and i_{invq} based on the prediction model, the defined cost function, and the constraints as described in the MPC formulation section. The MPC was implemented in MATLAB/Simulink using CasADi, which is an open-source tool for non-linear optimization and algorithmic differentiation [12]. The IPOPT nonlinear solver was used to solve the optimization problem.

TABLE I
SUMMARY OF SIMULATION PARAMETERS

Parameters	Values	Parameters	Values
R	0.08 Ω	Sample time (T_s)	0.1 ms
L	0.22 mH	Horizon length (N)	50
C	220 μF	Base voltage in $dq0$ frame	170 V

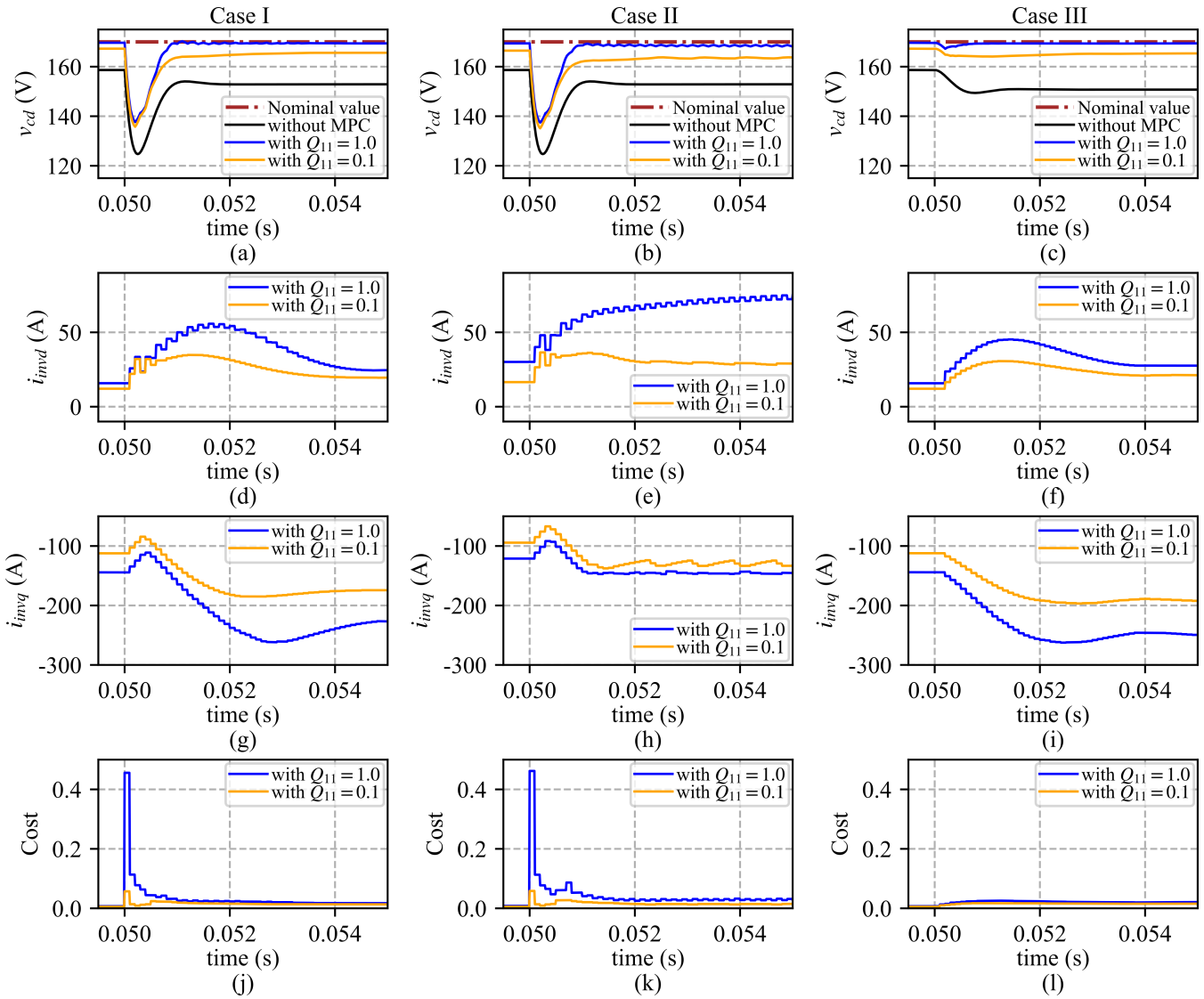

Fig. 3. Comparison of voltage support for different cases with different weighting parameters. Different columns represent different test cases. Different rows represents different variables: v_{cd}, i_{invd}, i_{invq} and cost in order.

V. Results and Analysis

The proposed MPC for voltage support was simulated for three different cases. For each of the case studies, the simulation results for two values of Q_{11} were analyzed. $Q_{11} = 1.0$ represents the case with higher priority for voltage support, and $Q_{11} = 0.1$ represents reduced priority for voltage support. In all cases, S_{11} and S_{22} were set to 0.01 and 0.001, respectively. Relatively smaller values of S_{11} and S_{22} were chosen compared to Q_{11} because it was considered that voltage support is a higher priority than minimizing the inverter current. Additionally, S_{22} was selected to be smaller than S_{11} because the cost of reactive power is less than active power and utilizing active power can cause ESS degradation.

Case I: Step change in load

In this case, v_g was set to 1 pu and a step load change from 0.5 pu to 0.7 pu is applied at $t = 0.05$ s. The magnitude of inverter currents i_{invd} and i_{invq} both were limited to 300 A, i.e., $I_{d,max} = I_{q,max} = 300$ A. Fig. 3(a) shows the plot of v_{cd} for two values of $Q_{11} = 1.0$ and $Q_{11} = 0.1$ along with nominal value and without MPC. Without MPC, the voltage deviates significantly from the nominal value with 17.11 V of steady-state deviation from nominal. When MPC is used, the steady-state deviation is reduced to 0.59 V and 4.49 V for $Q_{11} = 1.0$ and $Q_{11} = 0.1$, respectively. The steady-state deviation is smaller for $Q_{11} = 1.0$ compared to $Q_{11} = 0.1$. Figs. 3(d) and 3(g) show the plot of i_{invd} and i_{invq}, respectively. Both d and q components of inverter current are utilized to support the voltage. However, the magnitude of i_{invq} is higher than i_{invd} as the weight on the q component of current S_{22} is small compared to the weight of the d component current S_{11}. This means MPC tries to utilize reactive power over the active power to support the system voltage. Also, it can be observed that higher values of inverter current is utilized for $Q_{11} = 1.0$ than that for $Q_{11} = 0.1$. This is because for $Q_{11} = 1.0$ voltage support is given a higher priority compared to ESS cost/degradation in the MPC formulation. The square wave behavior in i_{invd} occurs because

TABLE II
SUMMARY OF THE RESULTS

Performance Metrics	Case I			Case II			Case III		
	without MPC	Q_{11}=1.0	Q_{11}=0.1	without MPC	Q_{11}=1.0	Q_{11}=0.1	without MPC	Q_{11}=1.0	Q_{11}=0.1
Voltage nadir (V)	124.73	137.65	135.76	124.73	137.45	135.13	149.39	167.22	164.08
Steady state v_{cd} (V)	152.89	169.41	165.51	152.89	168.19	163.55	150.74	169.39	165.35
Steady state deviation (V)	17.11	0.59	4.49	17.11	1.81	6.45	19.26	0.61	4.65
Steady state i_{invd} (A)	-	25.37	19.61	-	78.10	29.36	-	26.79	20.62
Steady state i_{invq} (A)	-	-238.71	-178.12	-	-148.04	-139.43	-	-253.57	-193.40

control signals only change at sample instants in the MPC. Minor oscillation occur between consecutive time-steps in i_{invd} because this work computes the Thevenin's equivalent voltages v_d and v_q using derivatives of i_d and i_q as described in Section III-A. This tends to amplify the high-frequency components of the signal. Ideally, these variables would be estimated using an estimator and is a part of the future work. Fig. 3(j) shows the cost function whose value increases at transient and then decreases to steady-state.

Case II: Step change in load with reduced current limits

In this case, all the settings are the same as Case I except the value of $I_{d,max}$ and $I_{q,max}$, which are now set to 150 A each. This represents the case where inverter size is reduced, a reduced amount of active power is available, or only a certain portion is available for voltage support, and the remaining capacity is utilized for other ESS stacked services. In this case, because the maximum inverter currents are limited to lower values, i_{invq} reaches the limit as illustrated in Fig. 3(h). This slightly impacts voltage support as can be seen in Fig. 3(b), where there is a slightly larger steady-state deviation compared to that of Case I. In this case, steady-state deviations are 1.81 V and 6.45 V for $Q_{11} = 1.0$ and $Q_{11} = 0.1$, respectively. From Fig. 3(e), it can be observed that higher i_{invd} is utilized because i_{invq} now reaches the constraint limit, and thus extra current for voltage support must come from i_{invd}. Because cost of i_{invd} is higher than that of i_{invq}, voltage support must be compromised. Fig. 3(k) shows the corresponding cost function for this case.

Case III: Step change in grid voltage

For this case, the load was set to 0.5 pu and the limits on both $i_{d,max}$ and $i_{q,max}$ are set to 300 A. The value of v_g was changed from 1.0 pu to 0.95 pu at $t = 0.05$ s, which models 5% change in the microgrid voltage. This can be seen from Fig. 3(c), where a significant steady-state voltage deviation of 19.26 V in v_{cd} is seen. When MPC is used, v_{cd} is closer to nominal, and steady-state voltage deviations are 0.61 V and 4.65 V for $Q_{11} = 1.0$ and $Q_{11} = 0.1$, respectively. When $Q_{11} = 1.0$, voltage is closer to nominal than for $Q_{11} = 0.1$ because of the higher priority for voltage support than ESS cost/degradation in the former case. Figs. 3(f) and 3(i) show plots of i_{invd} and i_{invq}, respectively. To increase the voltage, the inverter injects active and reactive power. In this case as well, it can be observed that a higher value of i_{invq} is utilized because of the aforementioned reason. Also, it can be seen that the value of inverter current is higher for $Q_{11} = 1.0$ than for $Q_{11} = 0.1$ for a similar reason mentioned in the previous cases. Fig. 3(l) shows the cost function. A summary of all the above cases is provided in Table II.

VI. CONCLUSIONS

This paper presented an MPC framework to provide dynamic voltage support for microgrids. A simplified model was derived to capture the voltage dynamics of a microgrid and was employed in the proposed predictive control framework. The controller performance was validated in a simulation study under step load and voltage changes. The controller showed to be able to provide good QoS for the benchmark studied during a large load transient. It was observed that the performance of voltage support varied depending upon imposed weight and constraints. Furthermore, based on the weights imposed, the proposed approach allows the ESS operator to strike the right balance between QoS and ESS cost/degradation.

VII. ACKNOWLEDGMENTS

The authors thank Dr. Rodrigo Trevizan from Sandia National Laboratories for the technical review of this paper.

REFERENCES

[1] M. Farrokhabadi, C. A. Cañizares, J. W. Simpson-Porco *et al.*, "Microgrid stability definitions, analysis, and examples," *IEEE Transactions on Power Systems*, vol. 35, no. 1, pp. 13–29, 2019.

[2] J. C. Vasquez, R. A. Mastromauro, J. M. Guerrero, and M. Liserre, "Voltage support provided by a droop-controlled multifunctional inverter," *IEEE Transactions on Industrial Electronics*, vol. 56, no. 11, pp. 4510–4519, 2009.

[3] J. W. Simpson-Porco, F. Dörfler, and F. Bullo, "Voltage stabilization in microgrids via quadratic droop control," *IEEE Transactions on Automatic Control*, vol. 62, no. 3, pp. 1239–1253, 2017.

[4] J. Mongkoltanatas, D. Riu, and X. LePivert, "H infinity controller design for primary frequency control of energy storage in islanding microgrid," in *2013 15th European Conference on Power Electronics and Applications (EPE)*, 2013, pp. 1–11.

[5] T. Vandoorn, B. Renders, L. Degroote, B. Meersman, and L. Vandevelde, "Voltage control in islanded microgrids by means of a linear-quadratic regulator," in *Young Researchers Symposium, Proceedings*. IEEE Benelux Chapter, 2010, p. 5.

[6] S. K. Sarkar, F. R. Badal, S. K. Das, and Y. Miao, "Discrete time model predictive controller design for voltage control of an islanded microgrid," in 3^{rd} *International Conference on Electrical Information and Communication Technology (EICT)*, 2017, 6 pp.

[7] J. B. Rawlings, D. Q. Mayne, and M. M. Diehl, *Model predictive control theory, computation, and design*. Nob Hill Publishing, 2017.

[8] B. P. Bhattarai, S. Paudyal, K. S. Myers, R. J. Turk, and R. Tonkoski, "Model predictive optimal dispatch of behind-the-meter energy storage considering onsite generation uncertainties," in *2018 IEEE Power Energy Society General Meeting (PESGM)*, 2018, pp. 1–5.

[9] Y. Shan, J. Hu, and J. M. Guerrero, "A model predictive power control method for pv and energy storage systems with voltage support capability," *IEEE Transactions on Smart Grid*, vol. 11, no. 2, pp. 1018–1029, 2020.

[10] U. Tamrakar, D. Copp, T. A. Nguyen, T. M. Hansen, and R. Tonkoski, "Optimization-based fast-frequency estimation and control of low-inertia microgrids," *IEEE Transactions on Energy Conversion*, pp. 1–1, 2020.

[11] G. A. Perdikaris, *Discrete-Time Systems*. Dordrecht: Springer Netherlands, 1991, pp. 139–234. [Online]. Available: https://doi.org/10.1007/978-94-015-7929-2_3

[12] J. A. E. Andersson, J. Gillis, G. Horn, J. B. Rawlings, and M. Diehl, "CasADi – A software framework for nonlinear optimization and optimal control," *Mathematical Programming Computation*, vol. 11, no. 1, pp. 1–36, 2019.